

A Review of Fe/Ni Doping Effects on Barium Strontium Titanate: Characterization and Insights

Reenu Jacob

CMS College Kottayam, Kerala

ABSTRACT

Recent advancements in research, fueled by modern technologies, have garnered significant attention. Perovskite barium strontium titanate (BST), when doped with metals, has emerged as a promising material with vast potential for various applications. UV spectral analysis of metal-doped BST reveals that tunable band gaps can be achieved by varying annealing temperatures. Furthermore, the dielectric properties and impedance characteristics of Fe/Ni-doped BST highlight its potential in applications such as multilayer capacitors, PTC thermistors, piezoelectric devices, and energy storage systems.

Keywords: doping, grain size, low frequency dielectric dispersion, hopping mechanism.

INTRODUCTION

Nano composite materials have garnered significant attention from researchers worldwide for various reasons. One key driver of this research is their potential application in next-generation electronic and photonic devices. Nanoparticles, due to their nanometer scale, exhibit unique properties, such as quantum effects, short migration distances for photo-induced holes and electrons in photochemical and photocatalytic systems, and enhanced sensitivity in thin-film sensors [1]. The properties of nanoparticles—whether optical, electrical, or magnetic—are directly related to their size.

The development of lead-free piezoelectric materials has also gained considerable attention due to environmental concerns. Following the discovery of ferroelectric ceramics in polycrystalline barium titanate [2], numerous new materials and technological advancements have led to a variety of industrial and commercial applications. If transition metals are doped with perovskites, their electronic structure will get dominated by the hybridization of the d-orbital. BaSrTiO₃(BST) has attracted substantial interest due to its perovskite structure and high dielectric constant [3], making it widely used in multilayer ceramic capacitors (MLCCs) and dynamic random-access memory (DRAM) systems [4].

Doping barium strontium titanate (BST) with metal ions significantly alters its properties and broadens its potential applications. A reduction in the grain size of BST is observed by the introduction of metal ion dopants is likely due to distortions caused by the differing ionic radii and the charge interactions between anions and cations. The restriction of macromolecular movement attributes to an increase in dielectric permittivity. Additionally, the electrical and optical properties of BST thin films improve because of the reduction in the band gap energy. While the increase in disorder and the reduction in grain size usually lower the dielectric constant, the relative dielectric constant can still increase due to enhanced spontaneous

polarization within the perovskite lattice. Metal ion doping also enhances the ferroelectric properties of BST by promoting the formation of oxygen vacancies. Notably, doping with metal has shown considerable potential for applications in electronics and energy storage.

OPTICAL AND DIELECTRIC STUDIES

Iron-doped BST synthesized using a solid-state reaction observes a structural transition from tetragonal to cubic phase [5]. Nickel-doped BST ($\text{Ba}_{0.7}\text{Sr}_{0.3}\text{TiO}_3$) with nickel mole ratios ranging from 0 to 1% (BSTN) via a sol-gel method showed that higher nickel doping improved the crystallinity of BSTN while reducing the crystallite size. The grain size of BST materials plays a crucial role in their applications. XRD patterns of NiO-doped BST found no significant changes in the phase compositions of the BST upon NiO doping. The addition of NiO facilitated the sintering and crystallization of BST, although the crystal structure and cell dimensions remained unchanged. The average grain size of BST decreased due to the addition of NiO [7]. Therefore, it can be summarised that doping BST with metal ions is essential for optimizing its morphology and enhancing its dielectric properties, making it more effective for a wide range of BST applications.

Keigo Suzuki et al. discuss the optical band gap of barium titanate nanoparticles using the quantum confinement model [8]. UV absorption and band gap studies of BST at different annealing temperatures [9] were reported and pointed that a decrease in the band gap energy of SrTiO_3 occurred with an increase in temperature [10]. Rashmi Rekha Negi's research on the effect of Ba^{2+} on strontium bismuth titanate [11] and investigation on the temperature dependence of the absorption coefficient and refractive index of BaTiO_3 proved another significant contribution [12]. The optical properties of SrTiO_3 with BaTiO_3 at various annealing temperatures [13] and optical properties of BaTiO_3 sintered at different temperatures provided valuable insights into the optical properties of new materials.

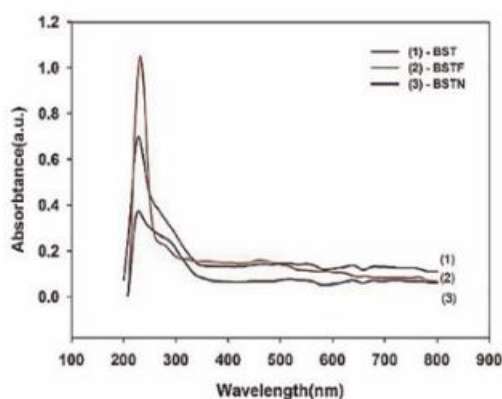


Figure 1(a): UV visible spectra of BST, BSFT and BSTN samples [5]

The optical band gap energy values affect the structure order-disorder in the degree of lattice of Fe doped Barium strontium titanate, BSFT ($\text{Ba}_{0.6}\text{Sr}_{0.4}\text{Fe}_x\text{Ti}_{(1-x)}\text{O}_{3-\delta}$, ($x=0.1, 0.4$)). Due to the substitution of Fe ion for Ti^{4+} creating Fe^{3+} ions, the band gap energy values show a marginal increase at higher temperatures (but lower than the band gap values of BST $\sim 3.93\text{eV}$) [14]. Addition of Fe, raises the fermi level above the conduction band edge resulting in an apparent

shift. This shift known as Burstein -Moss shift causes the widening of energy gap. This induces strain and varies the band gap energy values [15]. The energy band gap was found to increase with doping Fe into BST structure but the reverse trend was observed upon Ni doping where the band gap decreased with doping Ni [5]. This study (Fig 1(b)) confirms that tunable band gaps can be attained by varying the annealing temperatures or increase in band gap energy enhances the dielectric properties of the material.

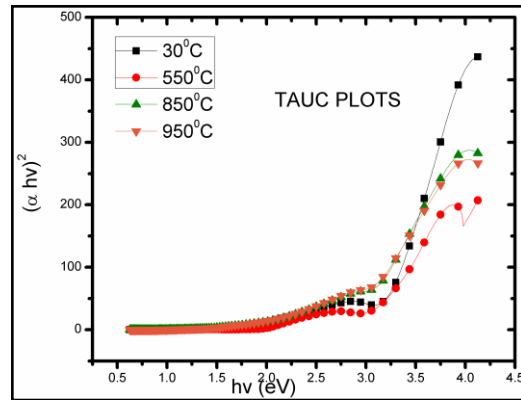


Figure 1(b): tauc plots of BSFT showing the variations in band gap energy [14]

Energy-Dispersive X-ray (EDX) analysis reveals the composition of the prepared ceramic powders (Fig 2).

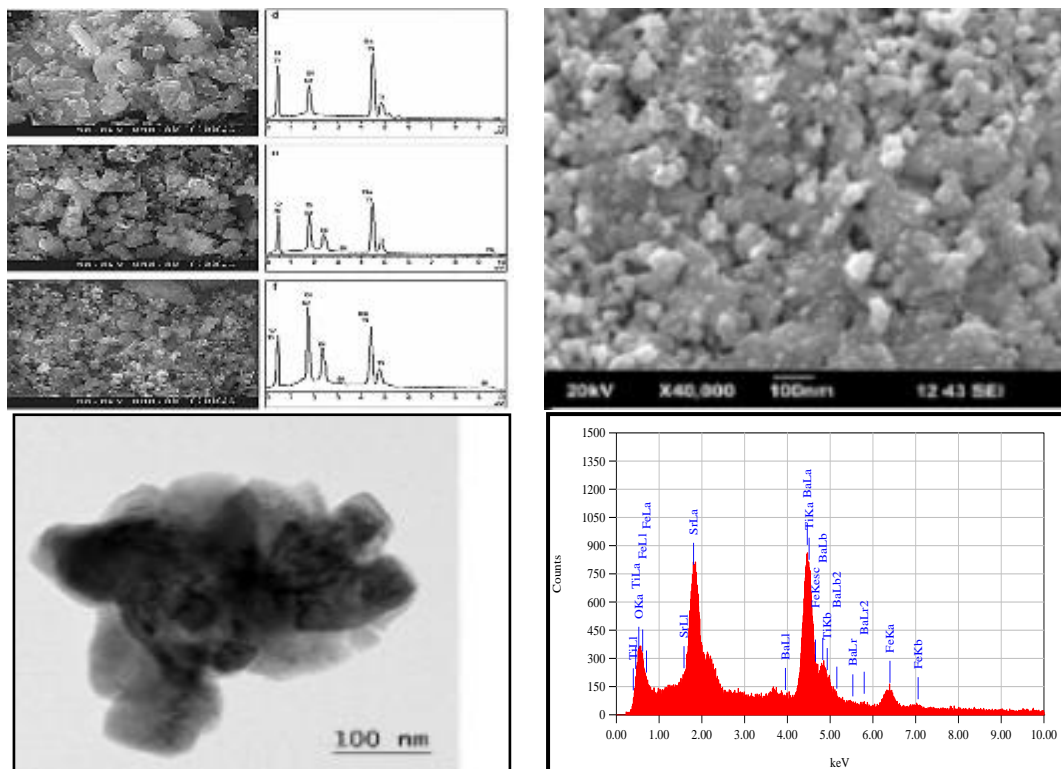


Figure 2: FESEM micrographs and EDXA analysis of (a) BST, (b) Bi-doped BST (2mol.% Bi), and (c) Bi-doped BST (4 mol.% Bi) and (d) Fe doped BST samples [4,6]

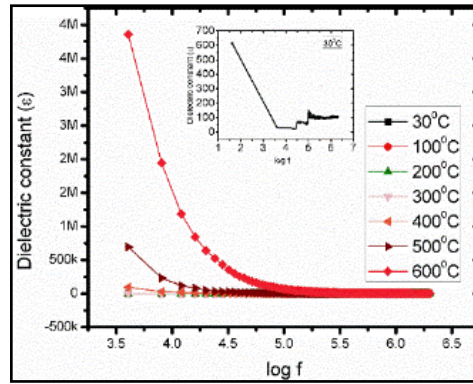


Figure 3(a): Frequency dependence of dielectric constant at different temperatures of BSFT($\text{Ba}_{0.6}\text{Sr}_{0.4}\text{Fe}_x\text{Ti}_{(1-x)}\text{O}_{3-\delta}$, ($x=0.1,0.4$)) [4]

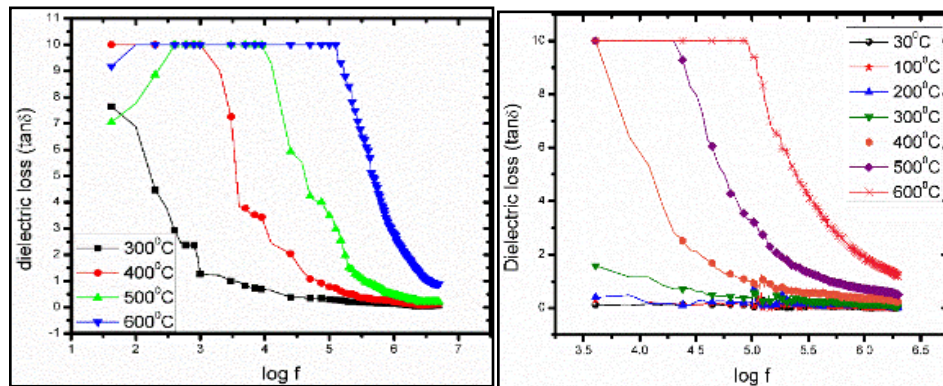


Figure 3(b): Frequency dependence of dielectric loss of at different temperatures BSFT($\text{Ba}_{0.6}\text{Sr}_{0.4}\text{Fe}_x\text{Ti}_{(1-x)}\text{O}_{3-\delta}$, ($x=0.1,0.4$)) [4]

The dielectric studies of (BSFT) show a decrease in the dielectric constant at low frequencies, attributed to Low Frequency Dielectric Dispersion (LFDD) (Fig. 3(a)). It is also evident that LFDD increases with temperature. The damping behaviour of these dipoles contributes to the reduction of the dielectric constant at higher frequencies. At elevated frequencies, orientational polarization becomes dominant [16], as the dipoles struggle to align with the rapidly changing field. The decrease in dielectric constant indicates the presence of a relaxation step within the material.

The broad peaks in the graph, depicting the variation of dielectric loss with frequency at different temperatures (Fig. 3(b)), indicate the non-Debye nature of the material. The elevated dielectric loss at higher temperatures is attributed to the DC conductivity within the material. A higher level of Fe substitution leads to a greater reduction in the dielectric parameters [14]. Acceptor doping of Fe^{3+} ions at the Ti^{4+} sites disrupts the Ti-O chains, leading to a reduction in the dielectric properties. The electrical modulus spectrum indicates that the electrical conduction in Fe-doped BST material follows a temperature-dependent hopping mechanism. In the high-frequency regions, a transition to a short-range conduction mechanism is observed. The real part of AC conductivity $\sigma_{ac} = \omega \epsilon_0 \tan \delta$, where $\omega = 2\pi f$ (f , the frequency used), $\tan \delta$ is the dielectric loss and ϵ_0 , the permittivity of vacuum. At higher temperatures, intrinsic factors influence the conductivity rate [18]. A sharp change in the conductivity curve slope is observed as the temperature increases, with the frequency at which this slope occurs corresponding to

the hopping frequency. The conductivity profile (Fig. 5) reveals low-frequency dispersion, an intermediate plateau, and high-frequency regions [4]. Thus, conduction is primarily governed by a hopping mechanism at lower temperatures and by quantum tunneling at higher temperatures. At very high temperatures, conductivity decreases, confirming the positive temperature coefficient (PTC) behavior of the BSFT sample.

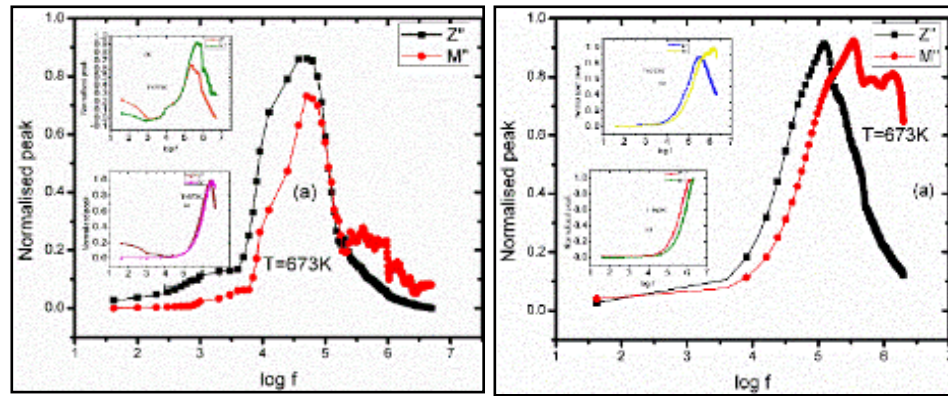


Figure 4(a): normalized imaginary parts of electrical modulus and impedance as a function of frequency for BSFT($\text{Ba}_{0.6}\text{Sr}_{0.4}\text{Fe}_x\text{Ti}_{(1-x)}\text{O}_{3-\delta}$, ($x=0.1,0.4$)) [14]

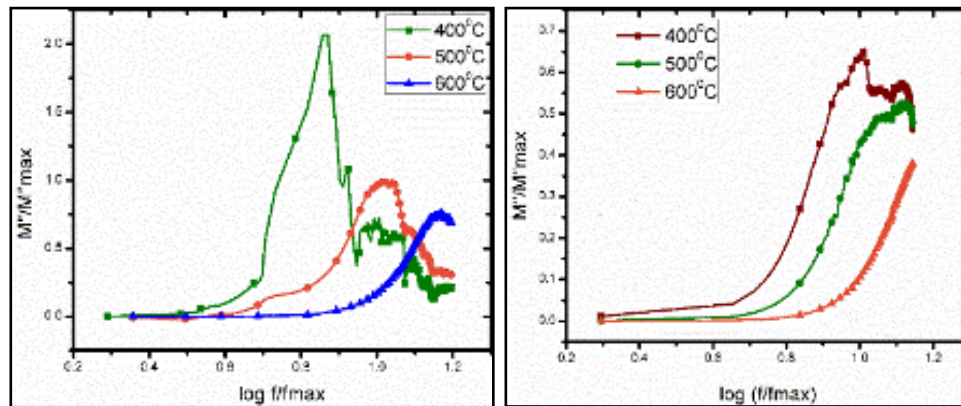


Figure 4(b): The scaling behavior of M'' at different temperatures for BSFT($\text{Ba}_{0.6}\text{Sr}_{0.4}\text{Fe}_x\text{Ti}_{(1-x)}\text{O}_{3-\delta}$, ($x=0.1,0.4$)) [14]

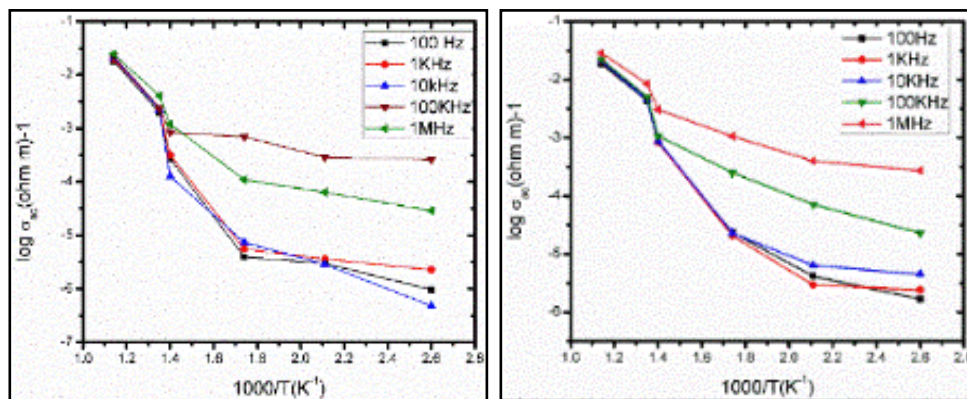


Figure 5: conductivity graph ($\log \sigma - 1/T$) of BSFT ($\text{Ba}_{0.6}\text{Sr}_{0.4}\text{Fe}_x\text{Ti}_{(1-x)}\text{O}_{3-\delta}$, ($x=0.1,0.4$)) at different frequencies [14]

The graph (Fig 4) displays a mismatch between the Z'' and M'' values at all temperatures. This indicates localized conduction showing the non-Debye nature. As the temperature increases the overlapping of curves becomes more pronounced. The combined plot of the normalized Z'' and M'' values with log frequency helps to understand whether short range or long-range charge carriers are playing the dominant role in the relaxation process.

The Cole-Cole analysis reveals the poly dispersive dielectric relaxation in the sample. The scaled coordinates ($M''(f, T)/M''_{\max}$ versus $\log(f/f_{\max})$), where f_{\max} is the loss peak frequency and M''_{\max} is the corresponding M'' value, are plotted (Fig. 4). If all the modulus loss profiles collapse into a single master curve, the relaxation process is temperature-independent [18]. However, a noticeable mismatch between the peaks indicates a temperature-dependent behavior. At very high temperatures, the curves show a slight merging tendency. This suggests that the conduction and relaxation processes in the Fe-doped BST sample involve similar charge barriers. The shape of the plot is influenced by the dielectric material, and defects, voids, and trapped charge carriers reduce the grain boundary resistances, subsequently affecting the conductivity of the material.

CONCLUSION

UV spectral analysis confirms that tunable band gaps can be achieved by varying annealing temperatures, with an increase in band gap energy enhancing the dielectric properties of the material. Impedance spectroscopy provides insight into the electrical transport mechanisms within the materials. The results confirm a hopping mechanism for the studied samples, supporting Jonscher's universal law. Depending on the applied electric field, the charge carriers transition between short-range and long-range hopping conduction. This also supports the polaron hopping mechanism, following the CBH model, at low temperatures. For the BSFT sample, at very high temperatures, the conductivity decreases, confirming the positive temperature coefficient (PTC) behavior. The results of conduction and relaxation processes show a strong correlation, indicating the involvement of similar charge barriers in both processes. The dielectric properties and impedance studies of Fe/Ni-doped BST make it a promising candidate for applications such as multilayer capacitors, PTC thermistors, piezoelectric devices, and energy storage devices.

References

- [1] Mishra, N. Mishra, et.al., Iron-doped BaTiO₃: Influence of iron on physical properties, *Int. J. Mater. Sci. Appl*, 2012.1: p. 14–21.
- [2] M. Mahesh Kumar, et.al., Dielectric relaxation in Ba_{0.96}Bi_{0.04}Ti_{0.96}Fe_{0.04}O₃, *J. Appl. Phys*, 1998.84: p.6811–6814.
- [3] M. Mahesh Kumar, et.al., Electrical and dielectric properties in double doped BaTiO₃ showing relaxor behavior, *J. Appl. Phys*, 1999.86: p. 1634–1637.
- [4] R. Jacob, et.al., Impedance spectroscopy and dielectric studies of nanocrystalline iron doped barium strontium titanate ceramics, *Processing and Application of Ceramics*, 2015.9: p.73–79.
- [5] Kaur, A. Singh, et.al., Structural, magnetic, and electronic properties of iron doped barium strontium titanate, *Rsc. Adv.* 2016,113: p.112363. DOI:10.1039/c6ra21458d.

-
- [6] A.D. Kakumani, et.al., Synthesis and characterizations of metal ions doped barium strontium titanate (BST) nanomaterials for photocatalytic and electrical applications, *Int. J. Appl. Ceram.Tec.* 2015. 13: p.177. DOI:10.1111/ijac.12421.
- [7] M. Banerjee, et.al., Synthesis and characterization of nickel oxide doped barium strontium titanate ceramics, *Cerâmica*. 2012. 58: .99. DOI:10.1590/s0366-9132012000100016 .
- [8] Pramod K Sharma, et.al., Structural ultraviolet shielding, dielectric and ferro electric properties of Ba_{1-x}Sr_x TiO₃(x=.35) thin films prepared by sole-gel method in presence of pyrole, *Thin Solid Films*, 2005. 91: p.204-211.
- [9] Eman M. Abid, et.al., Effect of Annealing Temperature on the Structural and Optical Properties of Nanocrystalline Strontium Titanate Thin Film Prepared by PLD, *International Journal of Innovative Research in Science, Engineering and Technology* ,2013.2: ISSN: 2319-8753.
- [10] Rashmi Rekha Negi et.al., The Effect of Ba²⁺ on Strontium Bismuth Titanate, Thesis, National Institute of Technology Rourkela-769008, p.2012-2013.
- [11] Al-Rasoul K. T, et.al., Structural and optical properties of BaTiO₃ thin films prepared by pulsed laser deposition, *Iraqi Journal of Physic*,2012.10: p. 41-44.
- [12] SupasaiT, et.al., Influence of temperature annealing on optical properties of SrTiO₃/BaTiO₃multilayered films on indium tin oxide, *Applied Surface Science*,2010.256: p.4462–4467.
- [13] Pankaj P. Khirade, et.al., Room temperature ferromagnetism and photoluminescence of multifunctional Fe doped BaZrO₃ nanoceramics, *Journal of Alloys and Compounds*,2017,691: p.287-298.
- [14] Reenu Jacob, Biofibre reinforced Ceramic polymer composites,2018, Thesis, Mahatma University.
- [15] Soumya Mukherjee, et.al, Synthesis and Characterization of Iron Doped Nano Barium Titanate Through Mechanochemical Route, *Journal of the Institution of Engineers (India): Series D* 94 2013.p.57–64.
- [16] Pournami P, et.al., Effect of calcinations on electrical properties of TiO₂ nanotubes, *Journal of Applied Physics* ,2012.112: p.104308.
- [17] Ali Omar Turkey, et.al., Tuning the Optical, Electrical and Magnetic Properties of Ba_{0.5}Sr_{0.5}Ti_xM_{1-x}O₃ (BST)Nano powders, *Physical Chemistry Chemical Physics*, RSC, DOI: 10.1039/x0xx00000x
- [18] Anumeet Kaur et.al., Electrical relaxation and conduction mechanisms in iron doped barium strontium titanate, *Ceramics International*,2018.44:p.204-21.